

Supporting Information

Addressing Sub-optimal Poses in Non-equilibrium Alchemical Calculations

Maurice Karrenbrock,[†] Valerio Rizzi,[†] Piero Procacci,[‡] and Francesco Luigi
Gervasio^{*,†,¶,§,||}

[†]*School of Pharmaceutical Sciences, University of Geneva, Rue Michel-Servet 1, CH-1206
Geneva, CH*

[‡]*Chemistry Department, University of Florence, Via della Lastruccia 3-13, 50019 Sesto
Fiorentino, IT*

[¶]*Institute of Pharmaceutical Sciences of Western Switzerland, University of Geneva,
CH-1206, Geneva, CH*

[§]*Chemistry Department, University College London (UCL), WC1E 6BT, London, UK*

^{||}*Swiss Bioinformatics Institute, University of Geneva, CH-1206, Geneva, CH*

E-mail: francesco.gervasio@unige.ch

5CF● 212-

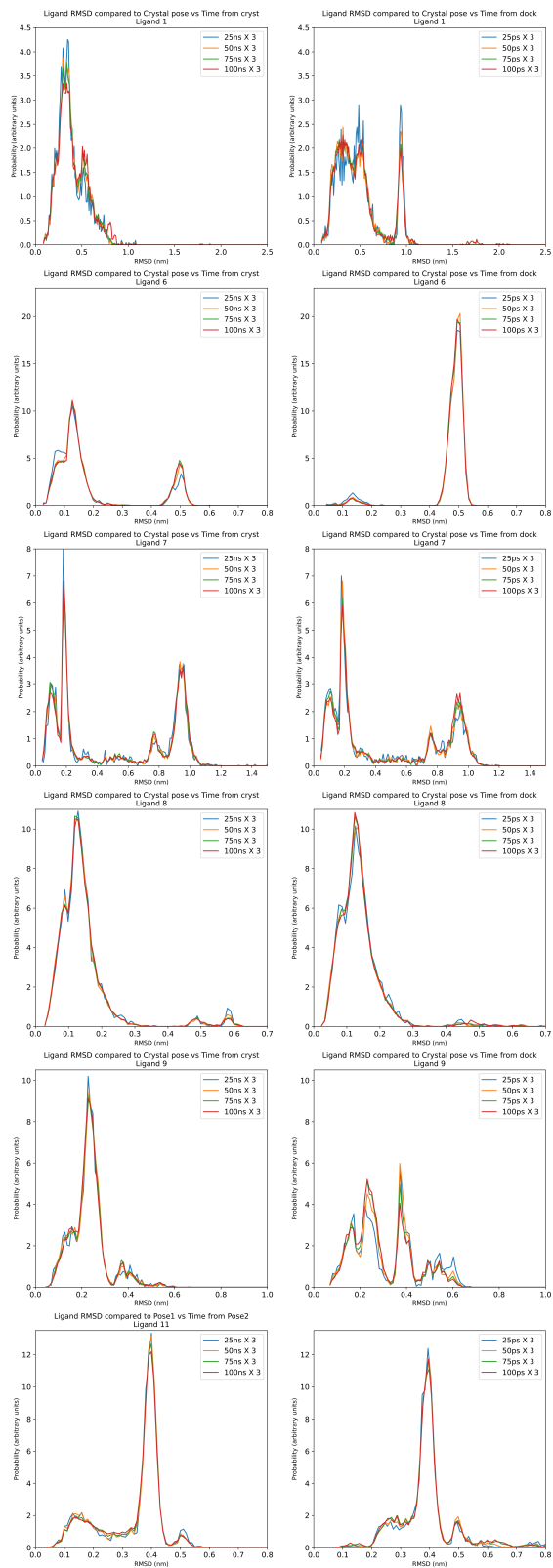


Figure S1: The evolution in time of the RMSD of the ligand compared to the crystallographic pose during the three independent 100ns HREM runs.

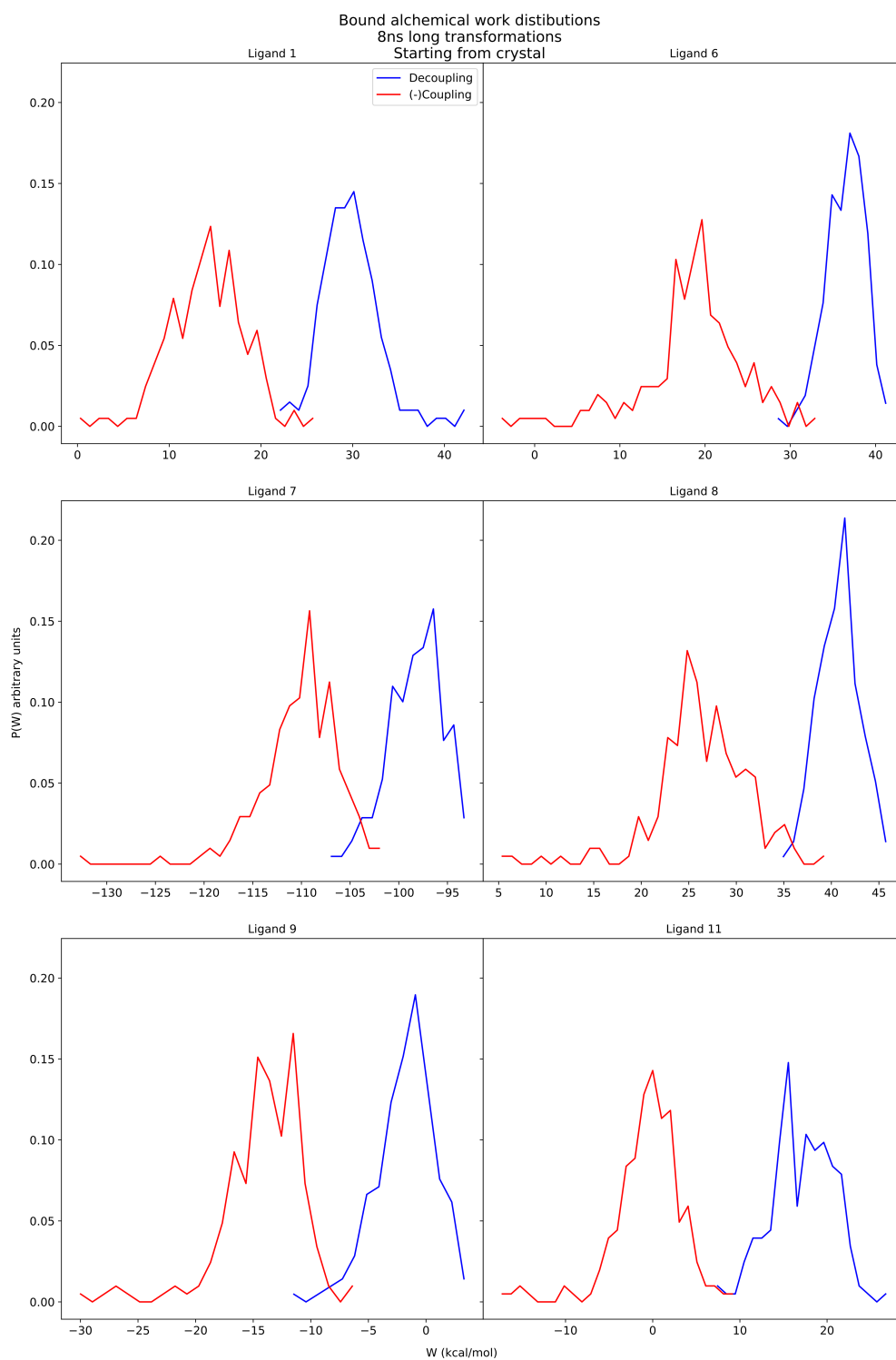


Figure S2: The probability distributions of the forward and backward processes for the 8ns long alchemical transformations of the ligand in the binding pocket (bound transformations) starting from the crystal pose.

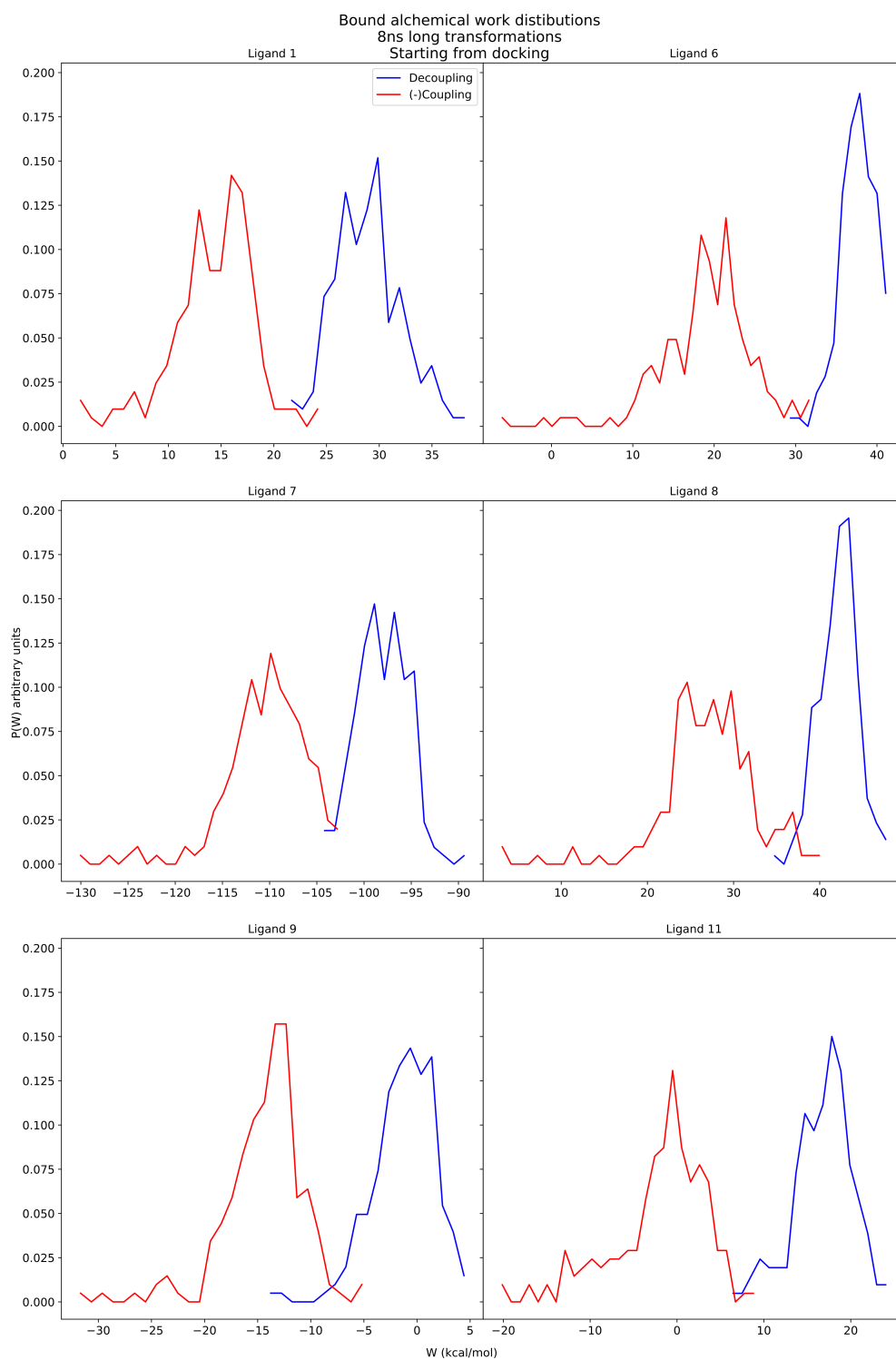


Figure S3: The probability distributions of the forward and backward process for the 8ns long alchemical transformations of the ligand in the binding pocket (bound transformations) starting from the docked pose.

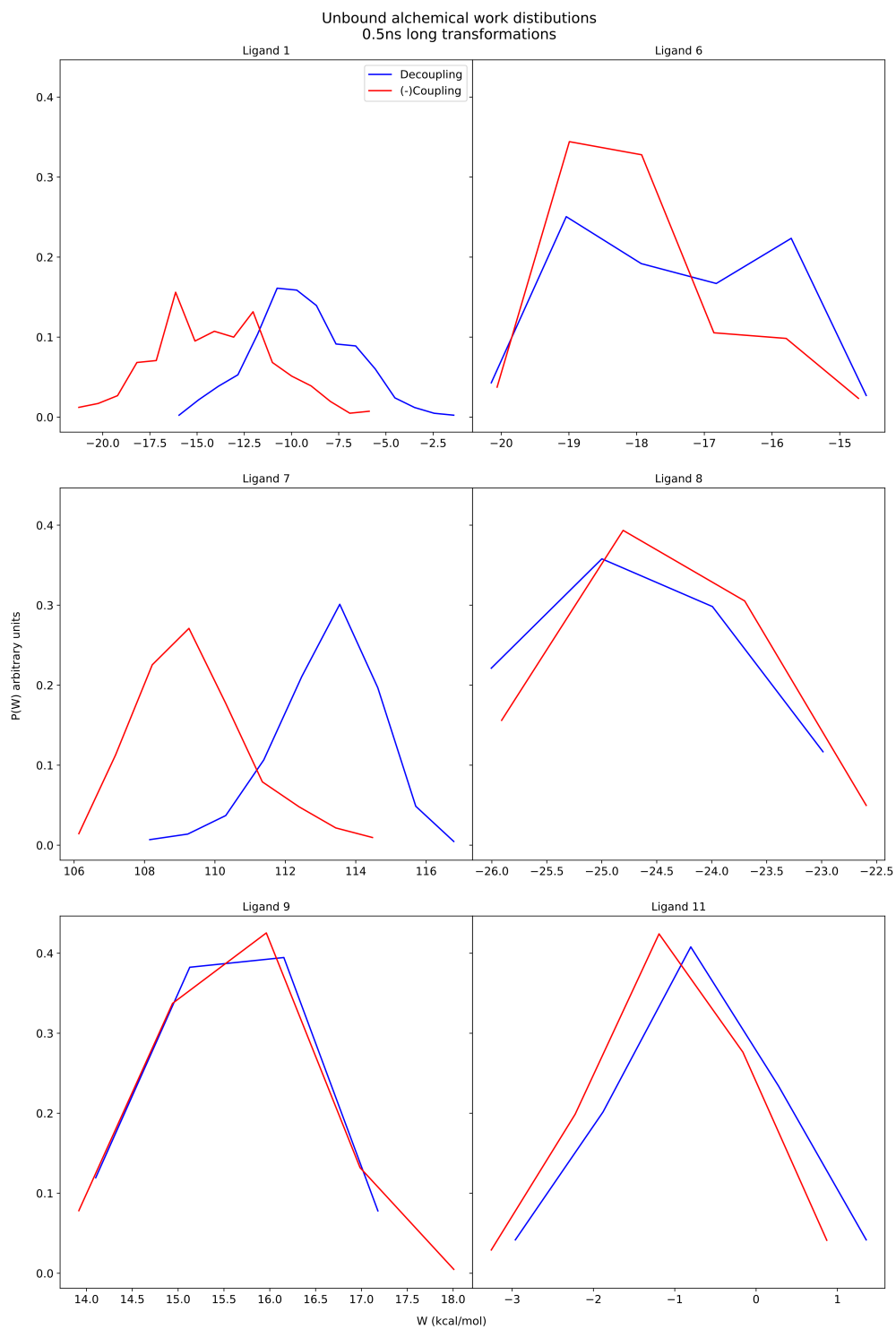


Figure S4: The probability distributions of the forward and backward process for the 0.5ns long alchemical transformations of the ligand in water (unbound transformations).

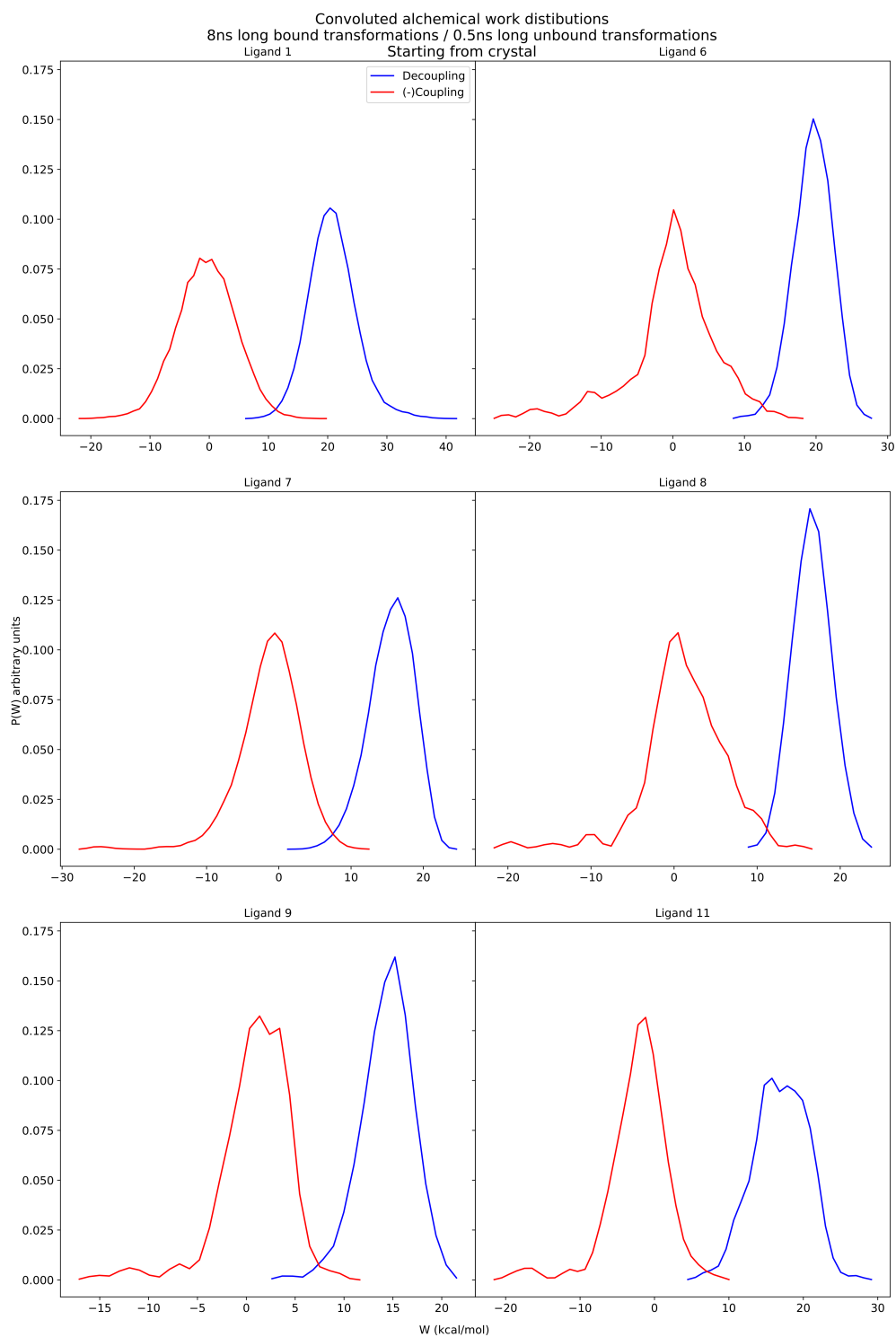


Figure S5: Combined probability distributions of the forward and backward process obtained with the convolution of the work values of the bound and unbound transformations, starting from the crystal pose.

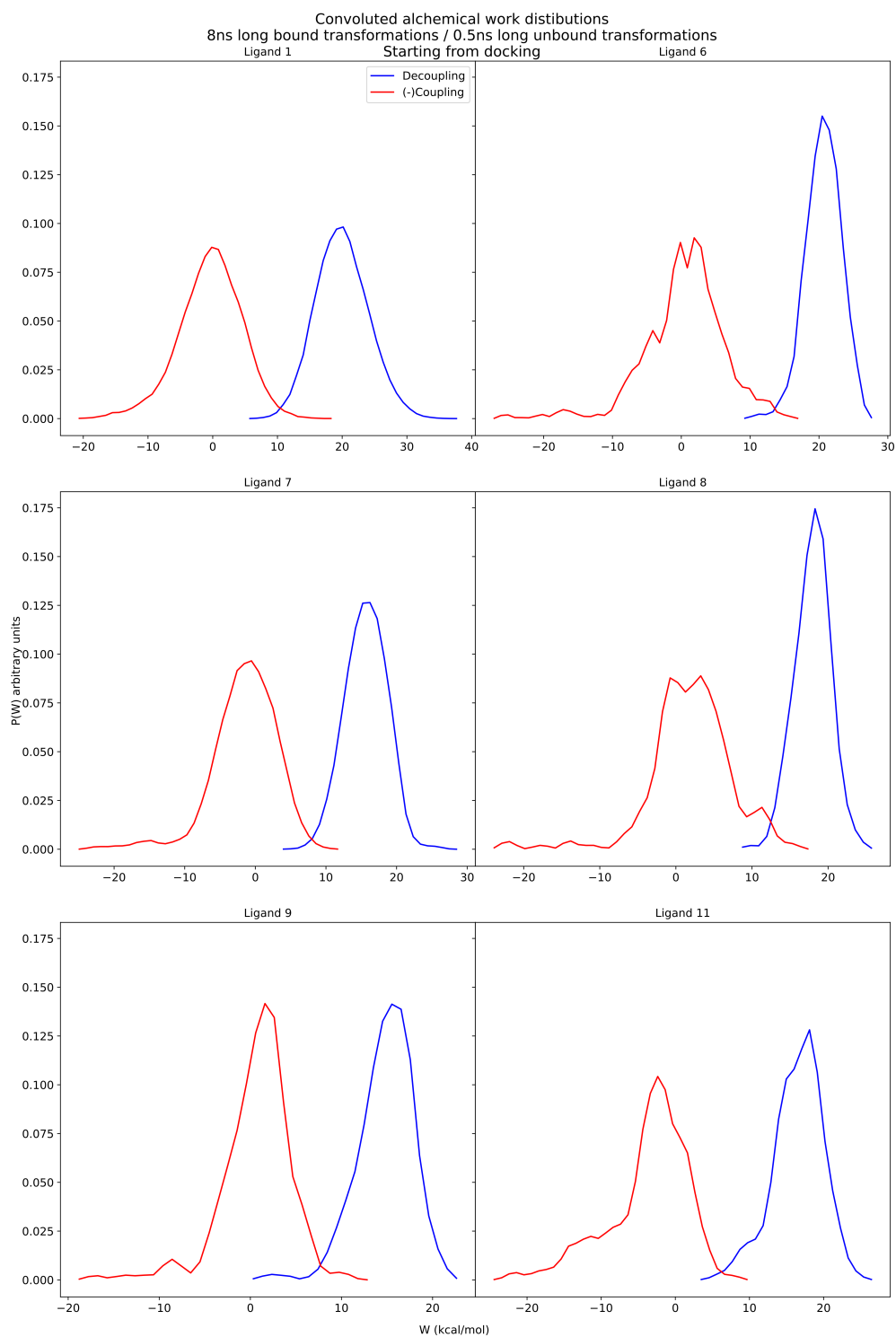


Figure S6: Combined probability distributions of the forward and backward process obtained with the convolution of the work values of the bound and unbound transformations, starting from the docked pose.

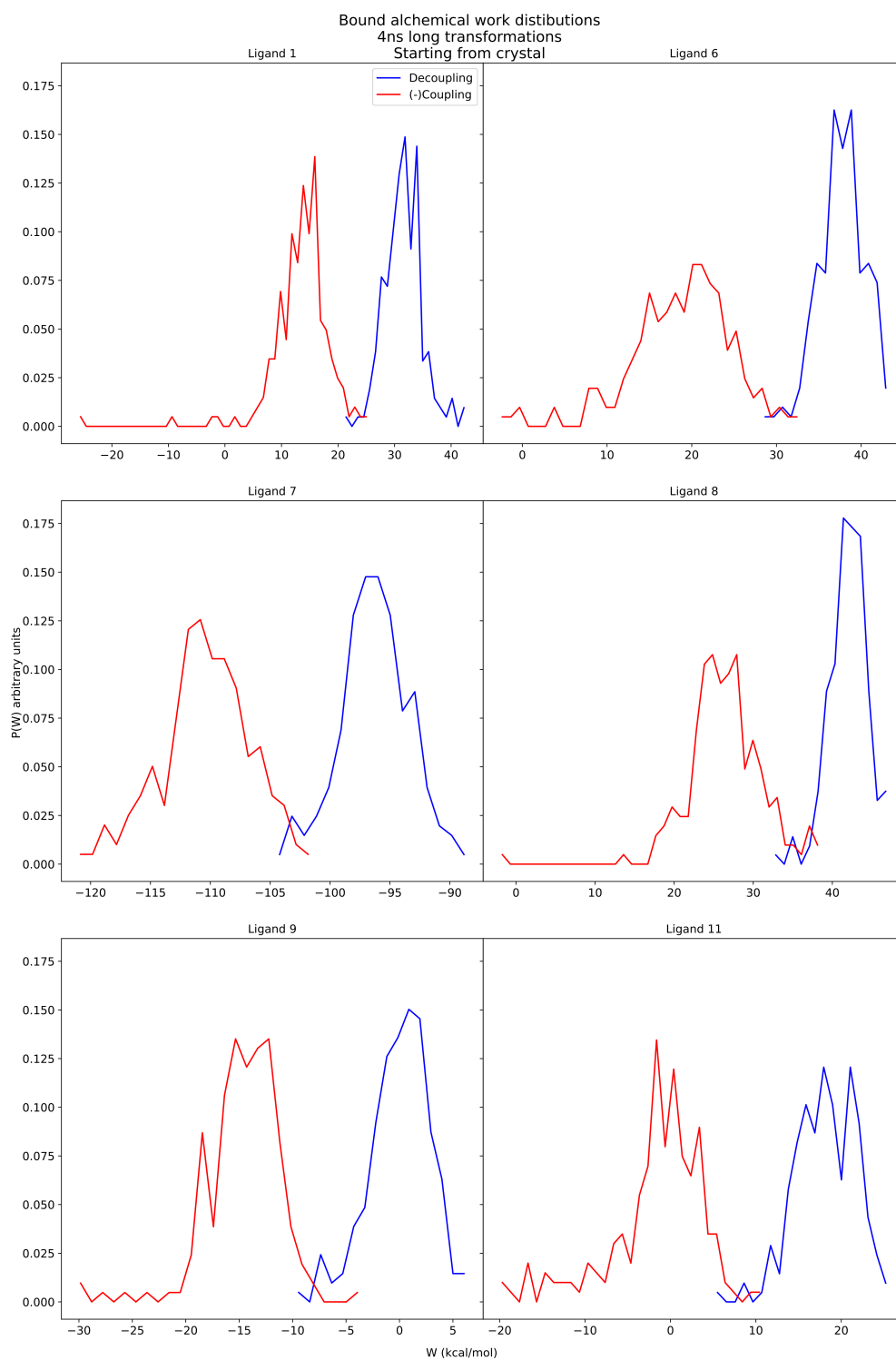


Figure S7: The probability distributions of the forward and backward process for the 4ns long alchemical transformations of the ligand in the binding pocket (bound transformations) starting from the crystal pose.

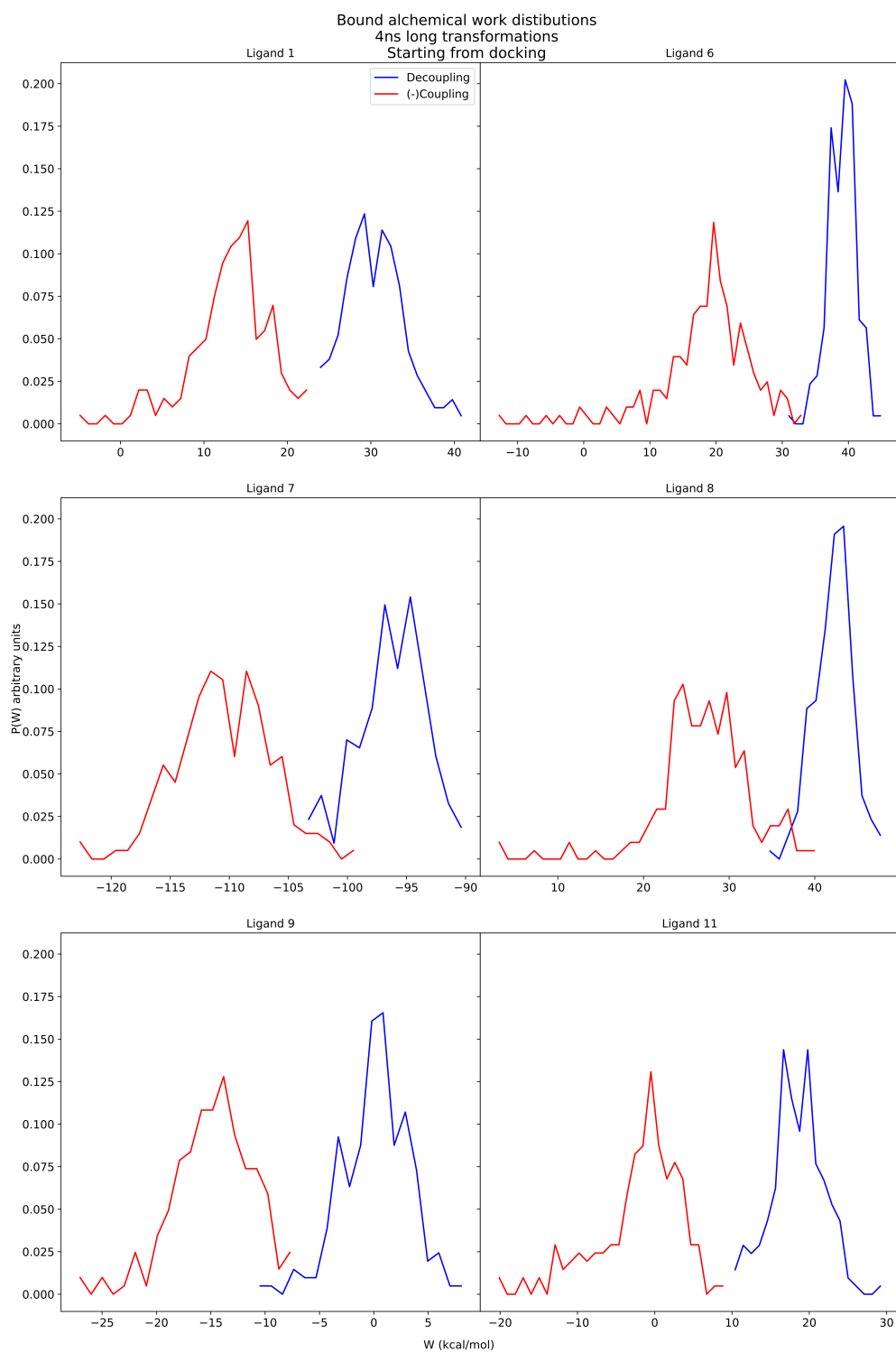


Figure S8: The probability distributions of the forward and backward process for the 4ns long alchemical transformations of the ligand in the binding pocket (bound transformations) starting from the docked pose.

Table S1: Free energy results in kcal/mol for the crystallographic pose, the docked pose without the convolution of the free alchemical work values.

Ligand	ΔG_{cryst}	ΔG_{dock}
1	7.8 +- 1.1	7.3 +- 1.0
6	9.2 +- 1.2	9.7 +- 1.3
7	4.0 +- 0.7	4.4 +- 0.5
8	7.8 +- 0.7	9.2 +- 0.7
9	4.0 +- 1.0	4.1 +- 1.1
11	3.7 +- 1.3	3.0 +- 1.2

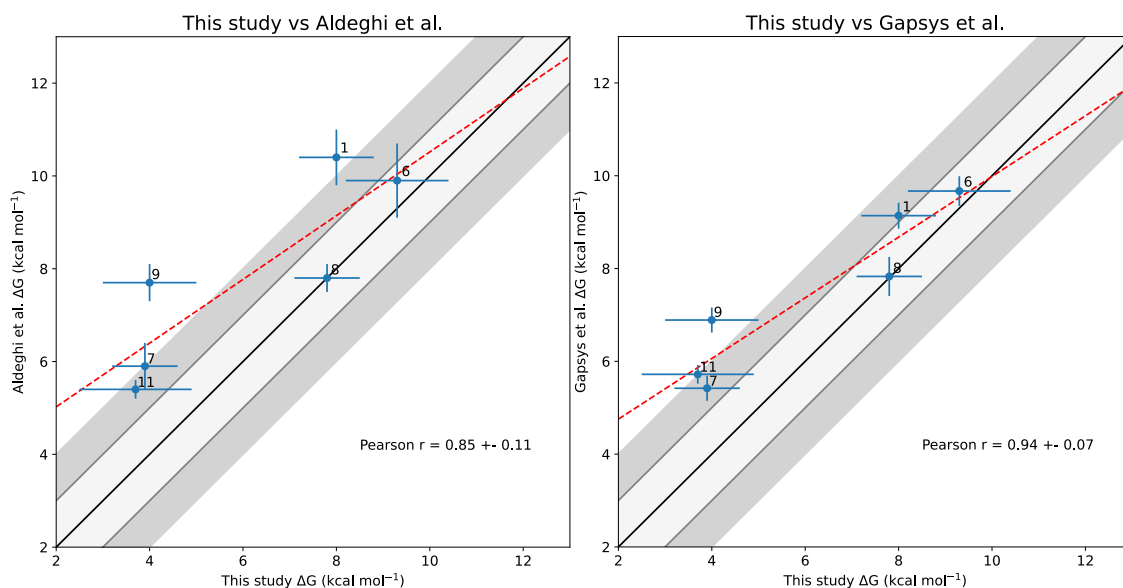


Figure S9: The results obtained in this paper on the crystallographic poses compared to the results obtained by Aldeghi et al.¹ and Gapsys et al.² The former uses FEP,³ while the latter performs bidirectional non equilibrium alchemical transformations.⁴⁻⁶

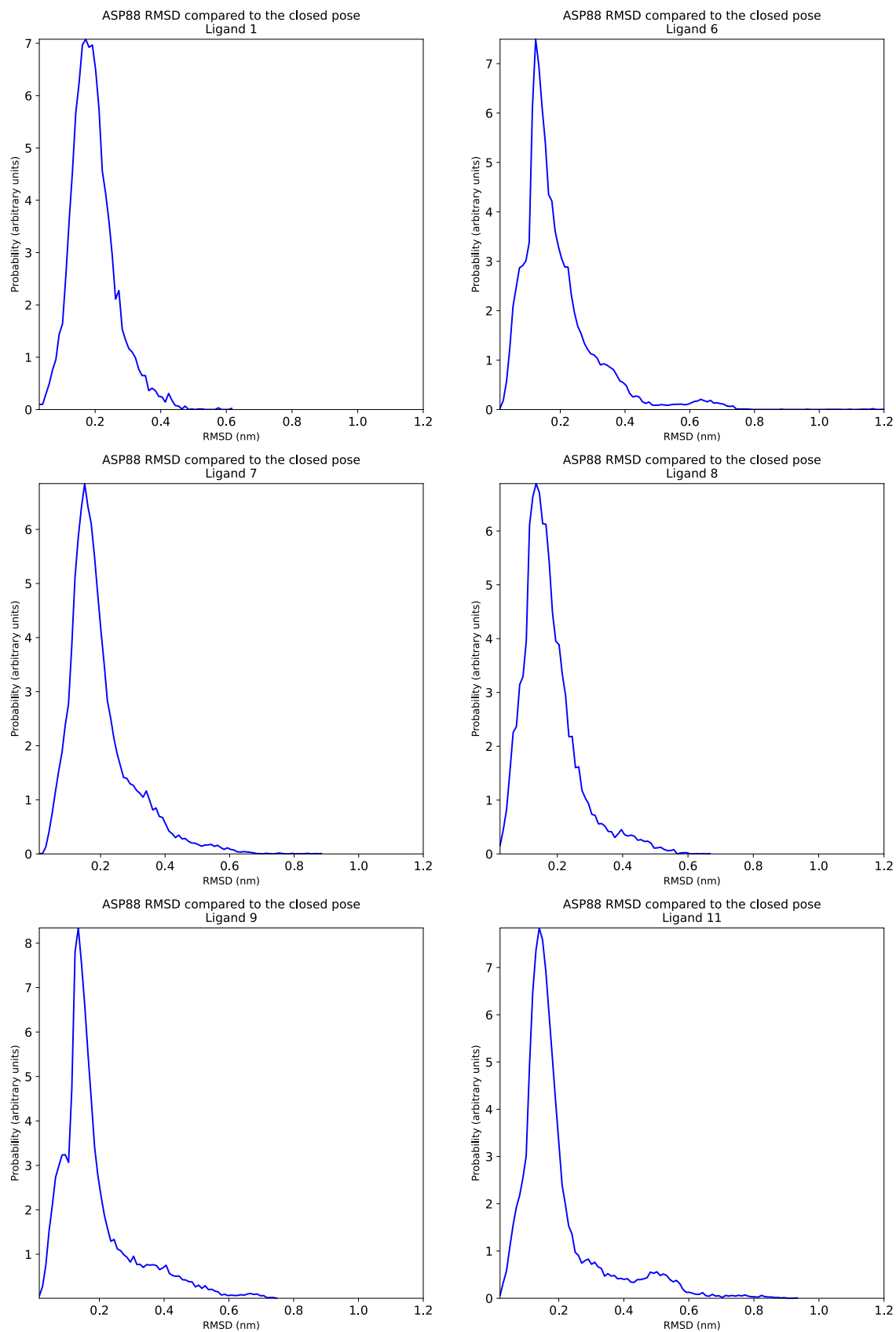


Figure S10: The probability distribution of the RMSD of residue ASP88 compared to the closed pose during the HREM for the HOLO structures.

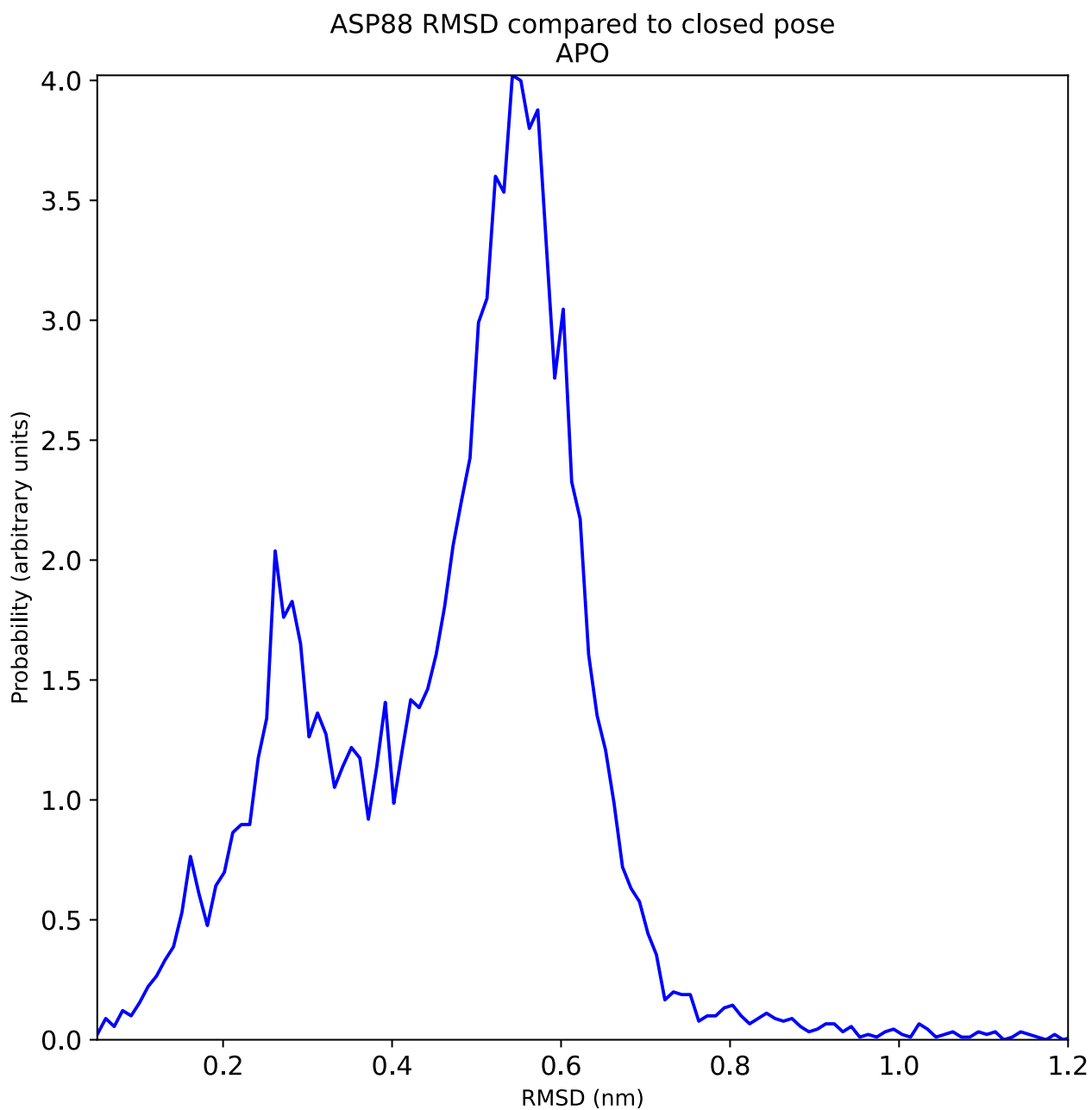


Figure S11: The probability distribution of the RMSD of residue ASP88 compared to the closed pose during the HREM for the APO structure.

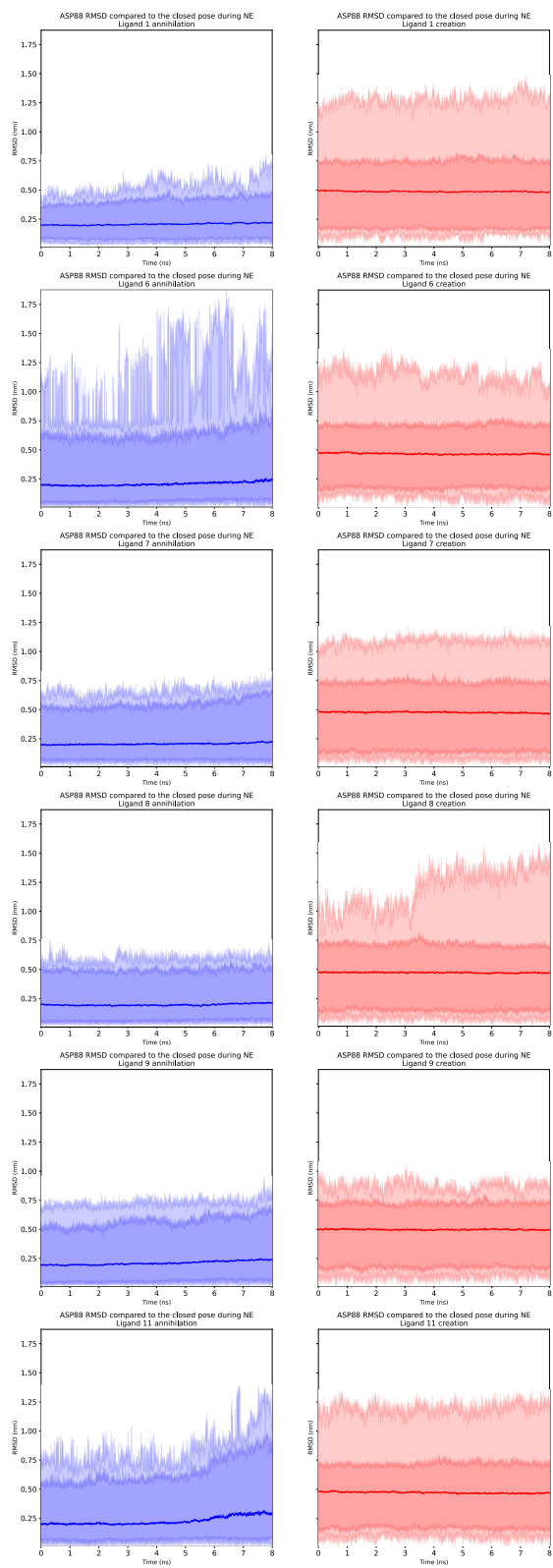


Figure S12: RMSD of residue ASP88 compared to the closed pose during the 200 non-equilibrium alchemical transformations. The line indicates the average value in time, the dark shaded region contains the 95% confidence interval, and the light shaded region is the area between the maximum and minimum value.

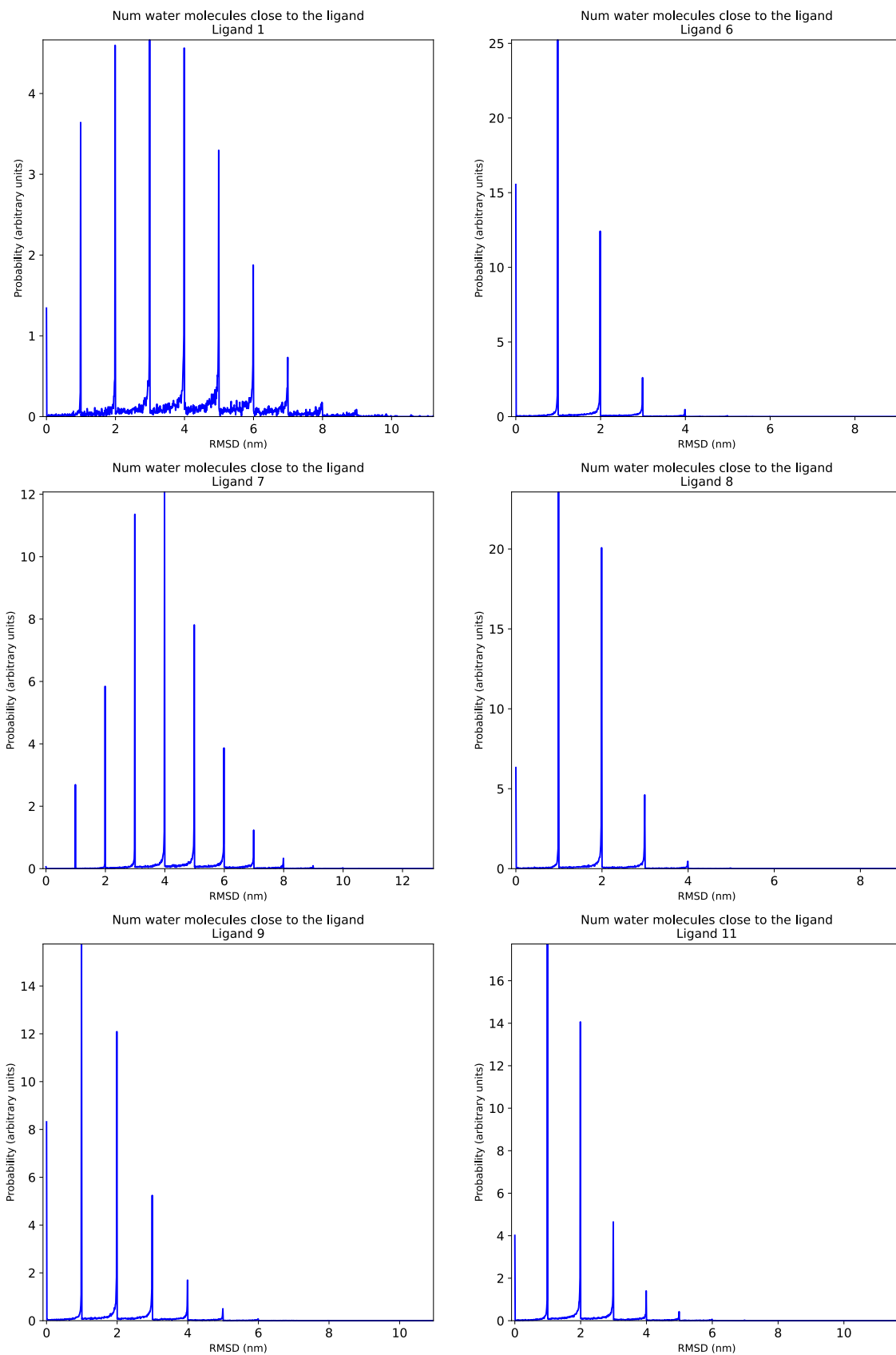


Figure S13: The number of molecules that are at maximum distance of 0.55nm from the center of mass of the ligand during the HREM of the HOLO structures.

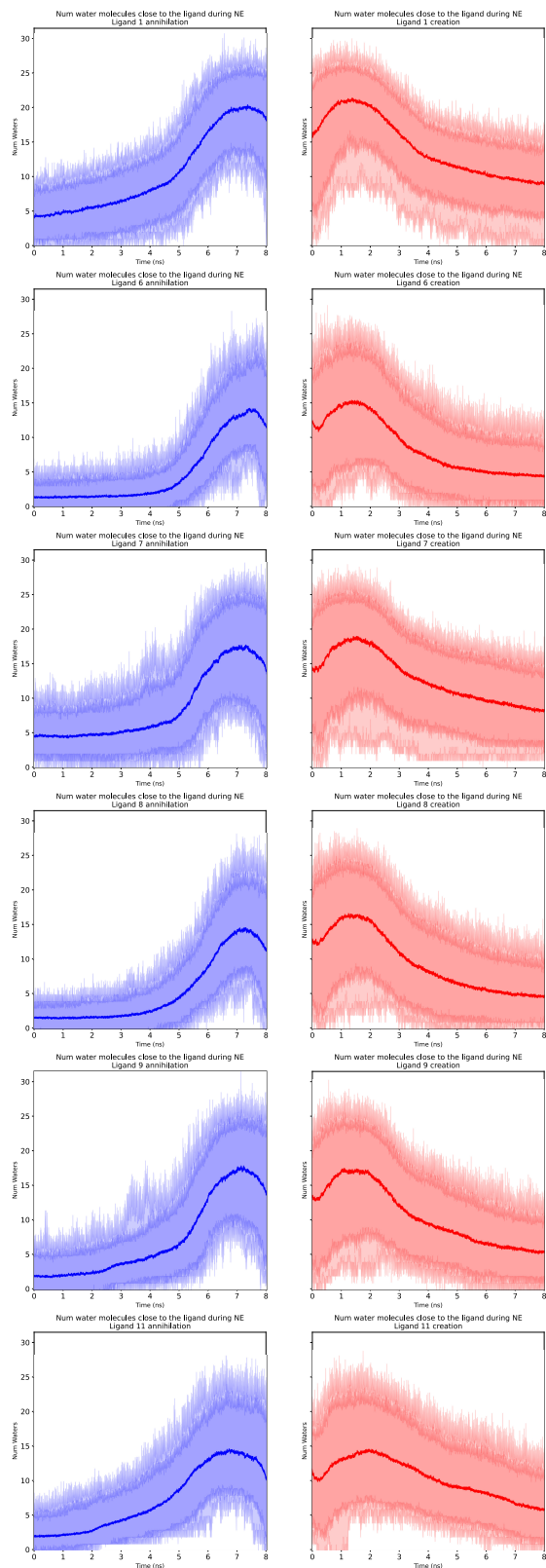


Figure S14: The number of molecules that are at maximum distance of 0.55nm from the center of mass of the ligand during the 200 non-equilibrium alchemical transformations, the line indicates the average value in time, the dark shaded region contains the 95% confidence interval, and the light shaded region is the area between the maximum and minimum value.

Table S2: The free energy results in kcal/mol for the crystallographic pose, and the docked pose calculated with Jarzynski’s equation⁷ on the ligand dissociation process.

Ligand	ΔG_{cryst}	ΔG_{dock}
1	8.8 +- 1.2	8.3 +- 1.1
6	11.9 +- 0.7	13.6 +- 0.5
7	7.5 +- 1.0	7.1 +- 0.7
8	9.9 +- 1.1	11.6 +- 0.5
9	6.5 +- 1.2	6.8 +- 1.0
11	6.3 +- 1.2	6.4 +- 1.0

References

- (1) Aldeghi, M.; Heifetz, A.; Bodkin, M. J.; Knapp, S.; Biggin, P. C. Accurate calculation of the absolute free energy of binding for drug molecules. *Chemical Science* **2016**, *7*, 207–218.
- (2) Gapsys, V.; Yildirim, A.; Aldeghi, M.; Khalak, Y.; van der Spoel, D.; de Groot, B. L. Accurate absolute free energies for ligand–protein binding based on non-equilibrium approaches. *Communications Chemistry* **2021**, *4*, 61.
- (3) Zwanzig, R. W. HighTemperature Equation of State by a Perturbation Method. I. Non-polar Gases. *The Journal of Chemical Physics* **1954**, *22*, 1420–1426.
- (4) Khalak, Y.; Tresadern, G.; Aldeghi, M.; Baumann, H. M.; Mobley, D. L.; de Groot, B. L.; Gapsys, V. Alchemical absolute proteinligand binding free energies for drug design. *Chemical Science* **2021**, *12*, 13958–13971.
- (5) Crooks, G. E. Path-ensemble averages in systems driven far from equilibrium. *Physical Review E* **2000**, *61*, 2361–2366.
- (6) Crooks, G. E. Nonequilibrium Measurements of Free Energy Differences for Microscopically Reversible Markovian Systems. *Journal of Statistical Physics* **1998**, *90*, 1481–1487.

- (7) Jarzynski, C. Nonequilibrium Equality for Free Energy Differences. *Physical Review Letters* **1997**, *78*, 2690–2693.